Electronic structure of ScN

G. Travaglini, F. Marabelli, R. Monnier, E. Kaldis, and P. Wachter
Laboratorium für Festkörperphysik, Eidgenössische Technische Hochschule Zürich, 8093 Zürich, Switzerland
(Received 24 February 1986)

The optical reflectivity has been measured over more than four decades of photon energy on chemically well-defined single crystals of ScN, in addition to the electrical conductivity and the Hall effect. From a Kramers-Kronig analysis the dielectric functions have been derived. A plasmon-phonon coupling (plasmaron) has been observed in the far-infrared region which could be decomposed and the phonon part of which compared with a Raman measurement of the phonon density of states. The interpretation of the optical results in a two-band model together with other data confirms recent theoretical estimates of the electron and hole masses and of the charge-carrier density in this compound, which we find is a compensated semimetal.

INTRODUCTION

The study of the electronic structure of the rare-earth-metal pnictides has again become a field of active interest.[1,2] On the theoretical side, the coexistence of localized $4f$ and extended band states makes a description of their excitation spectra by conventional *ab initio* methods unreliable,[3] and to avoid these problems, band-structure calculations are often performed for the pnictides with end members of the lanthanide series, i.e., La and Lu, or Sc and Y pnictides, which have empty or completely occupied $4f$ shells.[4–6]

The experimental situation is rather complex since in general it is still not known whether the rare-earth-metal pnictides are metals or semiconductors. However, up until now no rare-earth-metal pnictide has been shown to exhibit semiconducting behavior with respect to electric properties to our knowledge. Most of the pnictides have never been prepared as single crystals and only very few of them have been characterized by chemical analysis for their stoichiometry. In most of the investigated cases the concentration of the free carriers is a few percent of the cation concentration and thus of the same order of magnitude as the measured or expected off-stoichiometry. It therefore comes as no surprise that the literature is full of contradictory statements as to the semiconducting, semimetallic, or metallic nature of the rare-earth-metal pnictides.

All the rare-earth-metal pnictides (and chalcogenides) crystallize in the fcc rocksalt structure and thus symmetry considerations tell us that the anion p^6 valence bands have their maximum at the Γ point of the Brillouin zone. In this close-packed crystal structure the ligand field on the cation $5d$ orbitals is so large that the bottom of the conduction band will be formed by $5dt_{2g}$-derived and not by the $6s$-derived states. The $5d$ band has its minimum at the X point of the Brillouin zone. The question arises whether there is a gap between the p and the d band, resulting in an indirect-gap semiconductor, or whether there is an indirect overlap between the p and the d band, resulting in a semimetal.

To decide this point experimentally it is of utmost importance to have controlled (not only stated) stoichiometric, noncontaminated single crystals available. To our knowledge these conditions have been obtained only twice for GdP (Ref. 7) and GdN (Ref. 8) on which materials a multitude of measurements have been performed. Both compounds are semimetals with intrinsic carrier concentration of 7% and 6% per Gd ion, respectively.

Generally it can be said that the ionicity of the pnictides decreases from the nitride to the bismuthide and the increasing covalency shifts the anion p^6 valence bands to higher energies, favoring p-d overlap. Thus, of all compounds, the most likely to show semiconducting behavior are the nitrides.

In all rare-earth-metal pnictides, with the exception of the anomalous Ce compounds, the rare-earth-metal ions are in a trivalent state, as verified, e.g., by magnetic and neutron scattering experiments. As in the rare earth metals, the $4f$ states are between 2 and 10 eV below E_F (Ref. 9) and thus below the center of gravity of the p bands. As seen by second-order perturbation theory, the p-f interaction in this case will shift the p bands upwards, increasing the p-d overlap. Thus within the nitrides the compounds without occupied $4f$ states, i.e., ScN, YN, and LaN have the highest chance to become semiconducting. We have chosen for our investigation ScN because many contradicting band-structure calculations[4–6] and experiments[10–13] are available. The electronic structure calculations have recently been refined[14] resulting in a semimetal.

The first one to investigate the nitrides systematically was Sclar.[10] He made optical and electrical resistivity measurements and found in the case of ScN metallic resistivity on pressed-powder samples but postulated on the basis of optical transmission on evaporated films a semiconducting gap of 2.6 eV. He estimated in these samples a metal excess of about 10%. Busch *et al.*[11] used an optical powder re-emission technique for rare-earth-metal nitrides and observed for ScN an absorption minimum at 1.8 eV for a material having a nitrogen content of only 80% according to chemical analysis. Harbeke *et al.*[12] made optical reflectivity measurements between 1 and 12 μm on vapor-deposited epitaxial layers of ScN on Al_2O_3.

An absorption minimum for the best samples can be estimated at about 0.3 eV. They assume the material to be a semiconductor which had a measured carrier concentration of 1.5×10^{20} cm^{-3}, supposedly due to residual imperfections. Schlegel[13] made reflectivity measurements between 30 meV and 12 eV, for the first time on single crystals of ScN still having a metal excess of 5%. The carrier concentration was estimated to be 7×10^{21} cm^{-3} and the material was taken to be a semimetal. The absorption minimum was observed at 1.4 eV. It is thus clear that the position of the absorption minimum strongly depends on the stoichiometry and perfection of the material, being determined on the low-energy side by free-carrier absorption and on the high-energy side by interband transitions.

Several band-structure calculations are available for ScN, starting with that of Schwarz *et al.*[4] in which the potential was taken as a superposition of Hartree-Fock-Slater potentials for the neutral atoms, resulting in an insulator with an indirect gap of 3.38 eV. In their self-consistent calculation, again with the full Slater exchange, Weinberger *et al.*[5] found the gap reduced to less than 0.1 eV. In a later attempt by the same workers[6] the $X\alpha$ potential was used for exchange and correlation, with Schwarz's[15] atomic α values in the respective muffin-tin spheres, and $\alpha=\frac{2}{3}$ in the interstitial region. The result was a zero-gap material. The most recent investigation is that of Monnier *et al.*[14] Starting from a fully self-consistent linearized augmented plane wave (LAPW) calculation, with the von Barth—Hedin exchange-correlation potential, these authors included electron-hole correlation effects, which led from an initial value of 0.08 eV for the band overlap to a final value of 0.21 eV.

In order to clarify the situation experimentally we have thus gone through considerable effort to grow new and well-defined single crystals of ScN and to make optical reflectivity measurements over the largest available wavelength range. The results are then compared with the most recent electronic structure calculation.[14]

SAMPLE PREPARATION

Details of the experimental procedure have been described elsewhere.[16,17] The handling of the metal and compound has been performed in argon glove boxes gettered by hot cerium turnings, having a residual oxygen concentration less than 3 ppm. Turnings of 99.99% Sc metal have been reacted with nitrogen in an open molybdenum crucible for 12 h at 2000 °C. The resulting blue-grey material has been ground and then recrystallized for four days in electron-beam-welded, closed tungsten crucibles at a temperature of 2060 °C and a temperature gradient between top and bottom of 10 °C. This polycrystalline material was then transferred into another tungsten crucible and heated for five days to 2180 °C with a temperature gradient of 25 °C between top and bottom. At the bottom of the crucible, large single crystals of size (5 mm)^3 had grown.

The single crystals have been analyzed by a micro-Kjeldahl method for their nitrogen content. The crystals were extremely stable in air and moist atmosphere. In order to test for the metal content the crystals had to be boiled for many hours in a mixture of HNO_3 and H_2SO_4 to get dissolved. The final composition of the crystals used for optical measurements was $Sc_{0.503}N_{0.497}$ or $ScN_{0.99}$. The crystals had a green color and their lattice constant was 4.502 Å. Even after 24 h of x-ray irradiation only the rocksalt fcc phase could be detected.

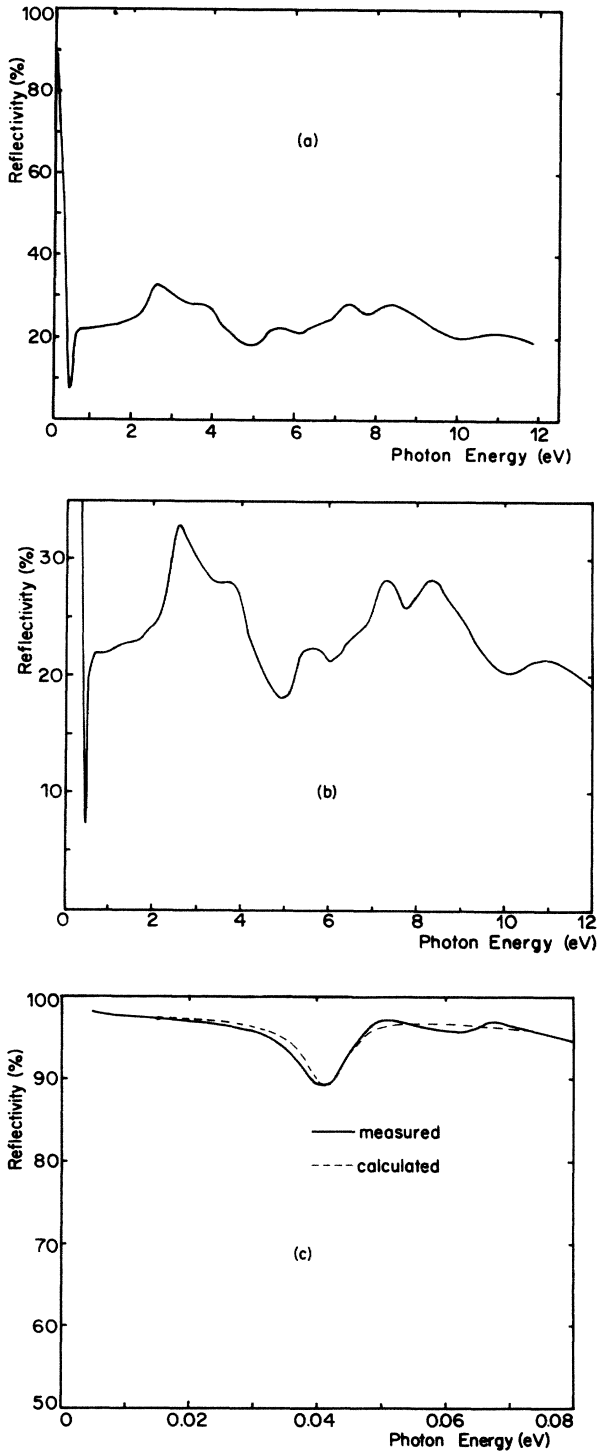

FIG. 1. (a) Near perpendicular reflectivity of ScN at 300 K. (b) High-energy region of the reflectivity of ScN. (c) Low-energy region of the reflectivity of ScN. Also shown is the calculated reflectivity from the self-consistent fit of the dielectric functions.

EXPERIMENTAL RESULTS

The optical reflectivity of ScN has been measured in a photon energy range from 12 eV down to 1 meV at room temperature using three spectrometers. In the uv and vacuum-uv ranges cleaved crystals have been used; in the infrared and far-infrared ranges polished surfaces had a higher reflectivity. In the far-infrared part of the spectrum we have employed a Fourier spectrometer with triglycene sulfate detectors down to 25 cm^{-1} and a liquid-helium-cooled germanium bolometer from 100 to 8 cm^{-1}. The whole spectrum is shown in Fig. 1(a), whereas in Figs. 1(b) and 1(c) the uv and far-infrared parts of the reflectivity, respectively, are shown in an expanded scale.

We also have measured the electrical resistivity by a conventional four-probe method and the Hall effect employing the van der Pauw technique. At room temperature σ_{dc} has been found to be 2.2×10^{16} sec^{-1} with a metallic temperature coefficient and the negative Hall effect implied a carrier concentration of $N_{eff}=5.9\times10^{20}$ cm^{-3} (Ref. 18) using an effective one-band model for the interpretation (but see discussion). The carrier concentration of our single crystals of ScN is thus close to the lowest one ever described.[12]

In order to get direct information on the phonon properties of ScN we measured also Raman spectra at ambient temperature with 5145-Å laser excitations. For reasons of comparison we investigated the neighboring-element compound TiN and also TiC because in this series, without greatly changing the masses of the ions, one can follow the screening effects of the charge carriers on the phonon modes. In these NaCl structures the first-order Raman effect is symmetry forbidden. Nevertheless the existence of defects relaxes the q-selection rule and the Raman effect measures a weighted one-phonon density of states (Fig. 2).

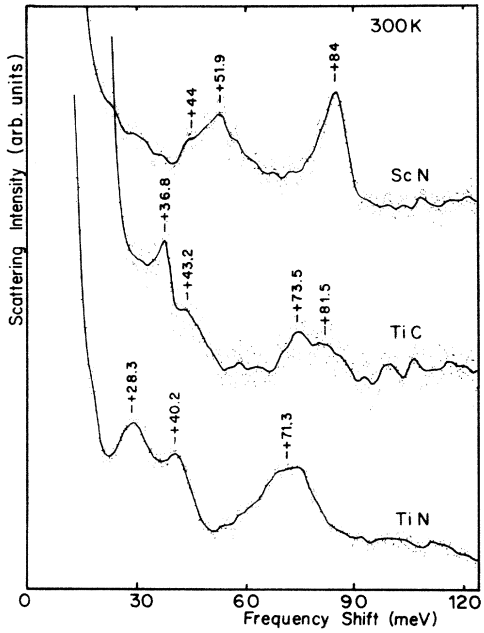

FIG. 2. Raman scattering of ScN, TiC, and TiN.

DISCUSSION

A Kramers-Kronig transformation of the reflectivity spectrum of Fig. 1(a) has been performed in order to obtain the optical constants ($\hat{\epsilon}=\epsilon_1-i\epsilon_2$, $\hat{\sigma}=\sigma_1-i\sigma_2$). The frequency range of the measured reflectivity spectrum has been extrapolated to zero frequency by means of the Hagens-Rubens relation

$$R(\omega)=1-(2\omega/\pi\sigma_{dc})^{1/2} \tag{1}$$

using the measured static value of the electric conductivity $\sigma_{dc}=2.2\times10^{16}$ sec^{-1}.[18] For energies larger than 12 eV and up to 18 eV the reflectivity has been assumed to drop off as ω^{-2}, and for still higher energies as ω^{-4}. The dielectric functions obtained are plotted for the high-energy range in Fig. 3 and for the low-energy range in Fig. 4. The real part (absorptive) of the optical conductivity is shown for the high-energy region in Fig. 5 and for the low-energy part in Fig. 6. The dielectric functions ϵ_1, ϵ_2, and σ_1 exhibit an interesting anomaly in the far-infrared region at about 45 meV (Figs. 4 and 6).

The analysis of the spectra is complicated by the fact that, besides the intraband absorption due to free carriers (Drude), TO phonons and high-energy interband transitions ($\rightarrow\epsilon_{opt}$), low-energy transitions of the holes between the different valence bands can take place.[19,20] In the approximation of Ref. 14, where the three cubically warped valence bands have been replaced by a nondegenerate band of light holes (mass m_L) and a doubly degenerate band of heavy holes (mass m_H), both isotropic, the energy range in which direct transitions occur is given by

$$[(m_H/m_L)-1]E_F^h \geq \hbar\omega \geq [1-(m_L/m_H)]E_F^h , \tag{2}$$

where E_F^h is the hole chemical potential. With the parameters of Ref. 14, this leads to 45 meV $\leq\hbar\omega\leq$ 115 meV.

Below this interval, each valence band has an independent free-carrier absorption, and the observed plasma frequency corresponds to

$$\omega_p^{low}=\left[4\pi e^2\left[\frac{2N_H}{m_H}+\frac{N_L}{m_L}+\frac{N_e}{m_{0e}}\right]\right]^{1/2} , \tag{3}$$

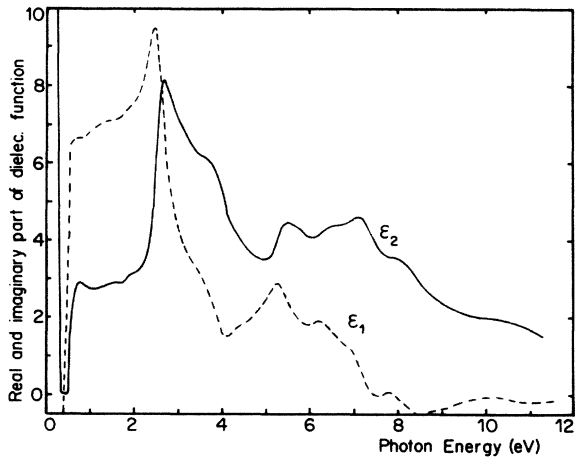

FIG. 3. Real and imaginary parts of the dielectric function of ScN.

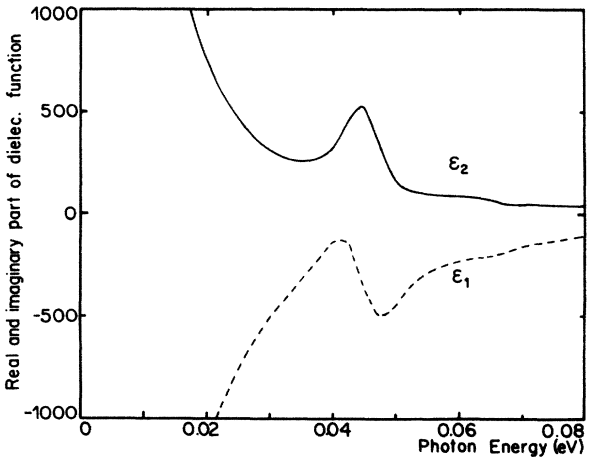

FIG. 4. Real and imaginary parts of the dielectric function of ScN in an expanded low-energy region.

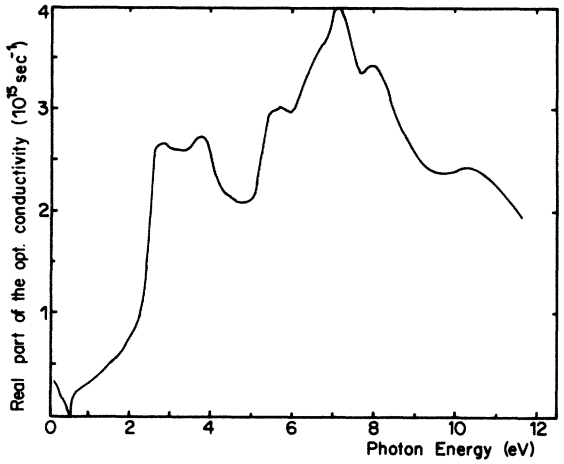

FIG. 5. Real part of the optical conductivity of ScN.

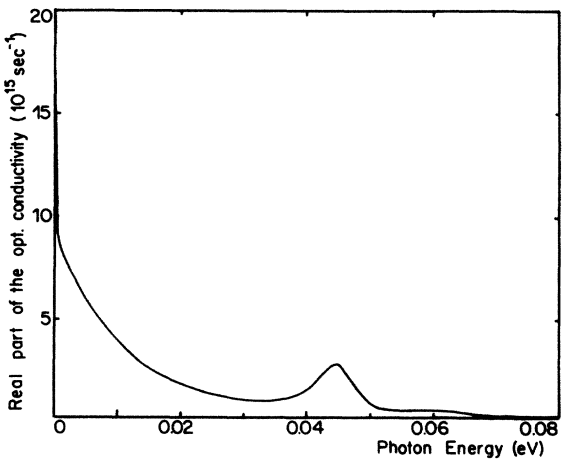

FIG. 6. Real part of the optical conductivity of ScN in an expanded low-energy region.

where $2N_H$ and N_L are the concentration of heavy and light holes, respectively, and $2N_H+N_L=N_e$ for a compensated system. m_{0e} is the optical mass of the electrons. In addition, the low-energy interband transitions will induce a positive correction to $\epsilon_1(\omega)$.

At higher frequencies than the above interval (but still smaller than the direct gap between valence and conduction bands), the response of the three valence bands combine into an effective Drude absorption, leading to a plasma frequency of the form

$$\omega_p^{\text{high}}=(4\pi e^2N_e/m_0)^{1/2}\ , \tag{4}$$

where m_0 is the optical mass of an electron-hole pair, defined in Ref. 14.

A realistic description of the optical response in the frequency range defined by Eq. (2) requires a calculation of the interband absorption within the valence-band complex. We have done this in the spherical approximation, using the equations derived by Combescot and Nozières (CN),[20] in which we have introduced a small damping term in order to suppress the unphysical divergencies in ϵ_1 due to the replacement of the true bands by their spherical component. The material parameters appearing in this modified $\epsilon_{\text{CN}}(\omega)$ were obtained from a fit of the dielectric functions at low ($\hbar\omega<80$ meV) frequencies to the formula

$$\hat{\epsilon}=\epsilon_{\text{opt}}+(\omega_p^{\text{low}})^2/(-\omega^2+i\gamma\omega) +\Omega^2/(\omega_{\text{TO}}^2-\omega^2+i\Gamma\omega)+\epsilon_{\text{CN}}(\omega)\ , \tag{5}$$

where ϵ_{opt} simulates the high-energy ($\hbar\omega>0.6$ eV) interband transitions; the second term is the contribution of the free carriers, the concentration of which can be obtained from Eq. (2), the neutrality condition $2N_H+N_L=N_e$, and the relation $N_H/N_L=(m_H/m_L)^{3/2}$; the third term is the absorption by a transverse optical phonon of frequency ω_{TO}, with a damping factor Γ and an oscillator strength Ω^2. Not included, but always present with lower probability, are indirect-hole interband transitions and indirect p-d interband transitions.

In the high-frequency range (200 meV $\leq\hbar\omega\leq$ 600 meV) we have modeled the dielectric function by the expression

$$\hat{\epsilon}=\epsilon_{\text{opt}}+(\omega_p^{\text{high}})^2/(-\omega^2+i\gamma\omega) +\Omega^2/(\omega_{\text{TO}}^2-\omega^2+i\Gamma\omega)\ . \tag{6}$$

The two fits produced values for ϵ_{opt} which differed by less than 5% from each other, and their average, $\epsilon_{\text{opt}}=5.2$, is less than half of the value 10.8 quoted in Ref. 12. The value there has been obtained by neglecting the absorption coefficient k (or ϵ_2) in the region for $\omega>\omega_p/(\epsilon_{\text{opt}})^{1/2}$ which, as seen in Fig. 3, is not permitted. Especially ϵ_1 exhibits a maximum of about 10 just in the region where one extrapolated the ϵ_{opt} value in Ref. 12. The real situation is therefore more complex and we find a fit procedure at lower energies than considered by Ref. 12 more reliable.

The splitting of ϵ_2 and ϵ_1 into its components according to Eq. (5) is shown in Figs. 7 and 8, respectively, and the reflectivity, computed from the fit is compared with the measured one in Fig. 1(c). The phenomenon which we encounter here is that of a typical plasmaron, i.e., a plasmon

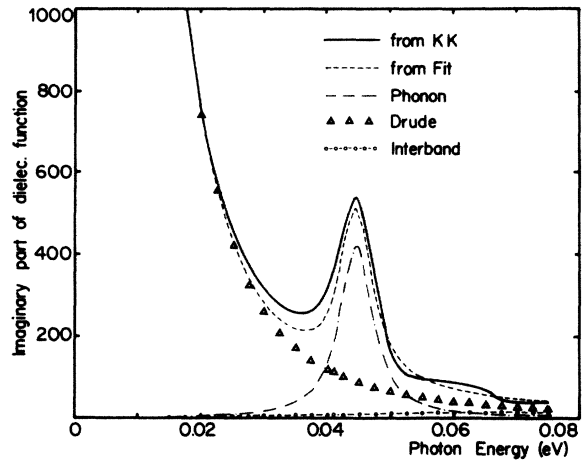

FIG. 7. Imaginary part of the dielectric function of ScN in the low-energy region. The figure shows the decomposition into the contributions given by Eq. (5). KK is the Kramers-Kronig transformation.

and LO-phonon coupling. The parameters which optimize the phonon part of the spectrum are $\omega_{TO}=45$ meV, $\Omega=380$ meV, and $\Gamma=7$ meV. Of the two components of the interband contribution, ϵ_{CN}, which depends on the carrier density, has to be compatible with the value for ω_p^{low}, which leaves a very small range of variation for ϵ_{opt}.

We also remark that $\epsilon_{CN}(\omega)$ adds a contribution of about 20 to the real part of the dielectric constant at zero frequency due to the interband transitions of the holes down to about 45 meV. The important aspect then is to realize that there must be optical absorption down to very low energies. It is exactly this absorption which has been neglected in Ref. 12. ω_{LO} can be obtained from the second zero crossing of ϵ_1 of the decomposed phonon part of Fig. 8 augmented by ϵ_{opt}. It amounts to 155 meV. In the absence of free carriers one can normally make use of the Lyddane-Sachs-Teller relation, connecting the static and optic dielectric constant with the longitudinal and transverse optical phonon frequency

$$\epsilon_{stat}=\epsilon_{opt}(\omega_{LO}/\omega_{TO})^2 . \tag{7}$$

We compute from Eq. (7) that ϵ_{stat} is 60, which can also be taken from Fig. 8. The interband transitions of the holes add to this about 20 so that the total dielectric constant for $\omega\rightarrow 0$ without the Drude term amounts to about 80.

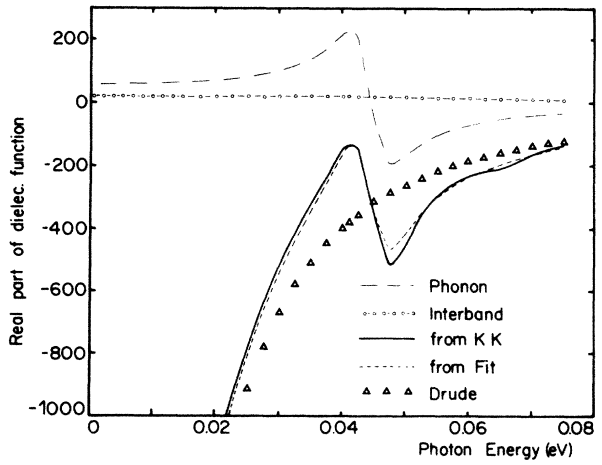

FIG. 8. Real part of the dielectric function of ScN in the low-energy region. The figure shows the decomposition into contributions given by Eq. (6). KK is the Kramers-Kronig transformation.

The phonon part of ϵ_1 in Fig. 8 can now be compared with the direct Raman measurements on ScN in Fig. 2. At first glance the figures bear little resemblance. As mentioned already above, the Raman effect in these fcc materials measures a weighted one-phonon density of states. The density of states is largest near the zone edges, thus the phonon frequencies taken from Fig. 2 correspond to values characteristic for the L point. The Raman spectra of TiN and TiC are in excellent agreement with density-of-states calculations.[21,22] Thus we can identify the Raman peaks at 28 and 40 meV in TiN and at 36 and 43 meV in TiC with the TA and LA modes at the zone edge, respectively. In ScN it is more difficult to discern between the TA and LA modes, the Raman peak is rather one broad structure centered at 52 meV. The density of states of the optical modes has only one peak both in the calculation and in the experiment and it is at 71, 74, and 84 meV for TiN, TiC, and ScN, respectively.

As can be seen from Fig. 2, the optical phonons as well as the acoustical phonons soften from ScN over TiC to TiN. This is in contrast to expectations from the lattice constant being 4.502, 4.329, and 4.24 Å, respectively, and suggesting rather a hardening of phonon modes. The softening of the acoustic modes from ScN over TiC to TiN is an effect of screening due to charge carriers. In ScN we have about 0.01 free carrier per cation (see below), in TiC about 0.15, and in TiN about 1.

The value we obtain for the transverse optical frequency of the decoupled phonon spectrum of Fig. 7 is with 45 meV strikingly low. The TO and LO modes of the decoupled phonon of Figs. 7 and 8 correspond to the Γ point because only there infrared transitions are possible. In other words the phonons in ScN taken from Figs. 2 and 7 cannot be compared directly. However, also in TiC,[22] ZrC,[23] and HfC,[24] which all have eight valence electrons per formula unit, as does ScN, there is an unusually strong reduction of ω_{TO} at Γ compared to the one at the L point. We attribute this to the strong electron-hole correlations in these systems,[14,25] which in terms of phenomenological parameters reflect themselves in a large polarizability of the ions and strong metal-ligand correlations.[26,27]

The most interesting parameters for our purpose are the two uncoupled plasma frequencies, which come out to be $\hbar\omega_p^{low}=0.82$ eV and $\hbar\omega_p^{high}=0.99$ eV ($\gamma\approx 0.01$ eV). From the latter frequency and the optical mass $m_0=0.13$ m given in Ref. 14, we find a density $N_e=9.3\times 10^{19}$ cm^{-3}, while from ω_p^{low} and Eq. (3) we obtain $N_e=6.6\times 10^{19}$ cm^{-3} and $N_H=0.44N_e$, $N_L=0.12N_e$. So the carrier concentrations obtained from the two fits are not exactly equal, but still rather close to each other. They are, however, 6 to 9 times smaller than the one obtained from the Hall effect measurement interpreted in terms of a single-

band model [$N_{\text{eff}}=5.9\times10^{20}$ cm^{-3} (Ref. 18)]. This is easily accounted for if one remembers that the charge transport takes place through several bands. Already in a two-band model, where the electrons have a mobility μ_e and the holes a mobility of μ_h, N_{eff} is renormalized by the factor $(\mu_e-\mu_h)/(\mu_e+\mu_h)$ to produce the true density. The holes have usually a smaller mobility than the electrons, and factors like the ones above are easily obtainable. We abstain from a further discussion of this point, since very little is known on the dominant scattering mechanism in ScN.

Consulting the self-consistent band structure of ScN (Ref. 14) or similarly that of Ref. 6 we observe that there is a lowest-energy direct p-d interband transition at the X point with an energy of 0.8 eV. It is exactly at this energy where we discern, best seen in ϵ_2 in Fig. 3, an absorption peak. The most prominent peak in ϵ_2 is at 2.6 and it corresponds to the direct transition at the Γ point. A very strong transition is also expected at the W point, because near this point the dispersion is flat and the energy bands are degenerate, leading to a high density of states. We observe this transition at 6.7 eV as the most prominent structure in Fig. 5. We refrain from going further into details of the interpretation of interband transitions up to 12 eV and rather wait until a computation of the dielectric functions from the band structure calculation becomes available.

We also made an x-ray photoemission spectroscopy (XPS) investigation of our ScN single crystals.[28] We observe a nonzero (but minute) density of states at E_F and two prominent peaks in the valence band spectra, separated by 10.5 eV. This corresponds exactly to the separation in energy of nitrogen $2s$ and $2p$ bands in the calculation of the density of states.[6] The peak with lowest binding energy, corresponding to the nitrogen $2p$ band, is found experimentally at 3.7 eV, and calculated at 2.7 eV.[6] Also the total width of the valence band is experimentally (resolution corrected) with 6.5 eV about 1 eV larger than the band-structure calculations would permit.[6,14]

Finally, looking at Fig. 5, we notice the sharp absorption minimum due to the screened plasma resonance at about 0.4 eV $\approx\omega_p^{\text{high}}/(\epsilon_{\text{opt}})^{1/2}$. For less perfect ScN this absorption minimum shifts appreciably into the near infrared region, up to even 2 eV. The measurements of the absorption minimum of Sclar,[10] Busch *et al.*,[11] and Schlegel[13] thus find their natural explanation.

From the dielectric constants we can also extract N^*, the effective number of electrons taking part in an optical transition

$$N^*=[m/(2\pi^2e^2)]\int^{\omega_{\max}}\epsilon_2\omega(\omega)d\omega\ . \tag{8}$$

Here $N^*=Nm/m^*$ for free carrier transitions, whereas the normal mass has to be used for interband transitions, whose oscillator strength f is obtained from the relation $N^*=Nf$. Looking at Fig. 9 we see two plateaus, one at about 0.2 eV, the other being approached near 12 eV. Considering the latter we find that interband p-d transitions originating in the $2p^6$ valence band of nitrogen become exhausted near 12 eV. The total number of electrons in this band is $N=4\times6/a^3=2.6\times10^{23}$ cm^{-3}. Comparing N with N^* we find f to be about 0.3, a reasonable oscillator strength for this transition.

Up to the plateau at about 0.2 eV we find transitions of free electrons near the bottom of the conduction band at X or holes near the top of the valence band at Γ and transitions of electrons near X to hole states near Γ. Apparently the band overlap is then about 0.2 eV, close to the theoretical value of 0.21 eV.[14] Decomposing the curve in Fig. 9 into a free carrier and interband contribution and then taking N^* from Fig. 9 to be about 7×10^{20} cm^{-3} and N_e to be 9.3×10^{19} cm^{-3} we get an m_0 of about $0.13m$, where we have to take into consideration that this is a mass averaged over all transitions. In this view this quantity is in good agreement with the theoretically derived value of $m_0=0.13m$ at the bottom of the band.

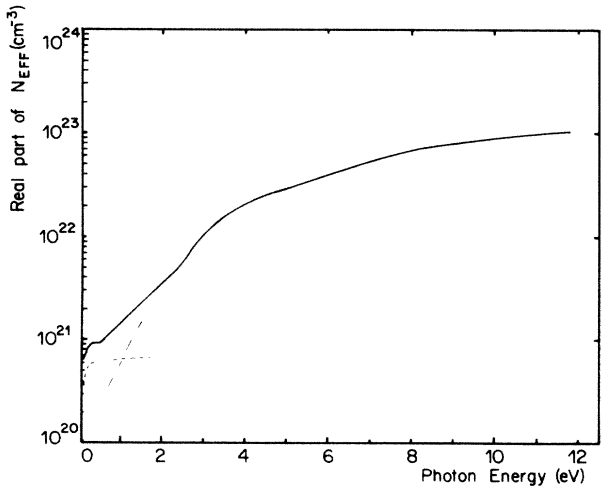

FIG. 9. Effective carrier concentration N^* of ScN.

CONCLUSION

We have given for the first time to our knowledge optical data over more than four decades of photon energy on chemically well-characterized, practically stoichiometric single crystals of ScN. The dielectric functions could be extracted from these data with great reliability. In the far-infrared region the plasmaron could be decoupled and phonon and carrier contributions could be separated. The data have been analyzed in a two-band model using light and heavy holes and electrons. The plasma resonance together with detailed electronic structure calculations, taking into account also electron-hole interactions, have permitted to make statements about the effective mass and the electron and hole concentrations. The fact that the experimental estimate of the carrier concentrations lies slightly below the theoretical ones strongly suggests that most of the observed charge is intrinsic. We thus can establish that ScN is a compensated indirect semimetal with a relatively low carrier concentration near 10^{20} cm^{-3}.

ACKNOWLEDGMENT

The authors are very grateful to Mrs. E. Jilek and A. Wisard for growing and chemically characterizing the single crystals. Many thanks are due to J. Müller for help in measuring the optical reflectivity. The authors acknowledge gratefully the conductivity and Hall effect measurements of B. Frick, the Raman measurements of I. Mörke, and the XPS measurements of T. Graf.

[1]A. Narita and T. Kasuya, J. Magn. Magn. Mater. **52**, 373 (1985).

[2]H. Harima and T. Kasuya, J. Magn. Magn. Mater. **52**, 179 (1985).

[3]H. L. Davis, *Conference on Rare Earths and Actinides,* Durham, N.C., Digest No. 2 (1971), p. 126.

[4]K. Schwarz, P. Weinberger, and A. Neckel, Theor. Chim Acta **15**, 159 (1969).

[5]P. Weinberger, K. Schwarz, and A. Neckel, J. Phys. Chem. Solids **32**, 2063 (1971).

[6]A. Neckel, P. Rastl, R. Eibler, P. Weinberger, and K. Schwartz, J. Phys. C **9**, 579 (1976).

[7]P. Wachter, E. Kaldis, and R. Hauger, Phys. Rev. Lett. **21**, 1404 (1978).

[8]P. Wachter and E. Kaldis, Solid State Commun. **34**, 241 (1980).

[9]P. A. Cox, Y. Baer, and C. K. Jorgensen, Chem. Phys. Lett. **22**, 433 (1973).

[10]N. Sclar, J. Appl. Phys. **35**, 1534 (1964).

[11]G. Busch, E. Kaldis, E. Schaufelberger-Teker, and P. Wachter, in *Les Éléments des Terres Rares,* Edition du CNRS, Colloque Internationle No. 180, Tome I (1970), p. 359.

[12]G. Harbeke, E. Meier, and J. P. Dismukes, Opt. Commun. **4**, 335 (1972).

[13]A. Schlegel, Ph.D. thesis, ETH Zurich, 1979.

[14]R. Monnier, J. Rhyner, T. M. Rice, and D. D. Koelling, Phys. Rev. B **31**, 5554 (1985). Using the values $\epsilon_{opt}=5.2$ and $\epsilon_{stat}=60$ of the present study, the equilibrium carrier concentration is predicted to lie between 1.8×10^{20} cm^{-3} (ϵ_0^* approximation) and 3.5×10^{20} cm^{-3} (rigid lattice approximation).

[15]K. Schwarz, Phys. Rev. B **5**, 2466 (1972).

[16]E. Kaldis and Ch. Zürcher, in *Proceedings of the 12th Rare Earth Research Conference,* edited by C. E. Lundin (Denver Research Institute, Denver, 1976), p. 915.

[17]E. Kaldis, B. Steinmann, B. Fritzler, E. Jilek, and A. Wisard, in *The Rare Earths in Modern Science and Technology,* edited by J. McCarthy *et al.* (Plenum, New York, 1982), Vol. 3, p. 224.

[18]B. Frick (private communication).

[19]D. Sherrington and W. Kohn, Phys. Rev. Lett. **21**, 153 (1968).

[20]M. Combescot and P. Nozières, Solid State Commun. **10**, 301 (1972).

[21]W. Kress, P. Roedhammer, H. Bilz, W. D. Teuchert, and A. N. Christensen, Phys. Rev. B **17**, 111 (1978).

[22]L. Pintschovius, W. Reichart, and B. Scheerer, J. Phys. C **11**, 1557 (1978).

[23]H. G. Smith, in *Superconductivity in d- and f-Band Metals,* edited by D. H. Douglas (AIP, New York, 1972), p. 321.

[24]H. G. Smith and W. Glaeser, Phys. Rev. Lett. **25**, 1611 (1970).

[25]G. Beni and T. M. Rice, Phys. Rev. B **18**, 768 (1978).

[26]W. Weber, H. Bilz, and V. Schroeder, Phys. Rev. Lett. **28**, 600 (1972).

[27]W. Weber, Phys. Rev. B **8**, 5082 (1973).

[28]T. Graf, Masters thesis, ETH Zürich, 1985.